RSC Advances

ROYAL SOCIETY OF CHEMISTRY

www.rsc.org/advances

Cite this: DOI: 10.1039/c0xx00000x

www.rsc.org/xxxxxx

ARTICLE TYPE

Green interfacial synthesis of two-dimensional poly(2, 5-dimethoxyaniline) nanosheets as a promising electrode for high performance electrochemical capacitors

Changzhou Yuan [a, c, *], Longhai Zhang [a], Linrui Hou [a], Jingdong Lin [b, *] and Gang Pang [a]

Received (in XXX, XXX) Xth XXXXXXXXX 20XX, Accepted Xth XXXXXXXXX 20XX
DOI: 10.1039/b000000x

2D poly(2, 5-dimethoxyaniline) nanosheets were first designed and tailored as intriguing pseudo-capacitive electrode for advanced supercapacitors *via* green interfacial synthetic strategy, and yielded large specific capacitance (SC) and remarkable SC retention at high rates in 1 M HCl electrolyte.

Recently, electrochemical capacitors (ECs) are gaining growing research interests worldwide, thanks to their attractive ability to deliver larger power density and longer cycling life than common rechargeable batteries, and energy density higher by orders of magnitude than conventional dielectric capacitors.[1] Among those typical electroactive materials for ECs, organic conducting polymers (CPs),[2-4] particularly polyaniline (PANI),[2, 4] has captured the extensive attention for the potential ECs application, owing to its low cost, easiness of synthesis, reversible control of electrical properties by charge transfer doping-dedoping and protonation, and intriguing pseudo-capacitive nature. To further enhance the processability of the PANI for commercial application, enormous efforts have been directed to the PANI derivates.[5] However, the substitution of groups in phenyl ring or N-position of PANI units commonly results in the decrease of the electronic conductivity,[6] which does not favor for the efficient energy storage, particularly at high rates. Fortunately, di-substituted poly(2, 5-dimethoxyaniline) (PDMA) with methoxy (-OCH_3) groups substituted at *ortho*- and *meta*- positions has shown high electrical conductivity similar to that of the PANI.[5, 7-10] Nevertheless, little has been reported about the PDMA for ECs so far, and furthermore, the PDMA samples were generally fabricated *via* chemical oxidative polymerization by using a variety of strong oxidants, e.g., $S_2O_8^{2-}$,[7] Fe^{3+},[9] a $S_2O_8^{2-}/Fe^{3+}$ binary oxidant.[5] As a consequence, it is of great significance but still a great challenge to explore facile yet efficient strategies by using greener and milder oxidants for fine fabrication of high performance nano-structured PDMA for advanced ECs.

Since interfacial polymerization method pioneer developed by Huang for controllable synthesis of classical PANI nanofibers,[11] elegant interfacial fabrication was extended well to prepare various CPs, and even CP-based composites by using the unique liquid-liquid interface of two immiscible liquids consisting of polar and apolar solvents.[2, 8, 12] The inhomogeneous and nanometer-scale interfacial region was endowed with unusual molecular aggregation and orientation, referenced to the bulk solution,[2, 8, 11-13], favoring for the fine construction of nano-structured materials. Unfortunately, some toxic organics (e.g., toluene, chloroform, CCl_4, *etc.*) were usually applied to build heterogeneous interface.[2, 11, 13] As a result, other environmentally-benign and green non-aqueous solvents were urgently expected for the efficient interfacial synthesis system.

Based on the above consideration, in the communication, we first developed an efficient water/ionic liquid (IL) green interfacial polymerization strategy (Fig. 1a and b) by using the H_2O_2 as appealing mild oxidant without any extra catalysts.[10] And the hydrophilic IL of 1-ethyl-3-methyl imidazolium tetrafluoroborate ([EMIM]BF_4) was applied here to build a prosperous interfacial platform for preparing novel two-dimensional (2D) PDMA nanosheets (NSs) with desirable electronic conductivity and large specific surface area (SSA). The as-obtained PDMA NSs were further utilized as an intriguing electroactive material for ECs. Strikingly, the as-fabricated 2D PDMA NSs delivered large specific capacitance (SC), and long-term electrochemical stability at large current densities in 1 M HCl aqueous electrolyte.

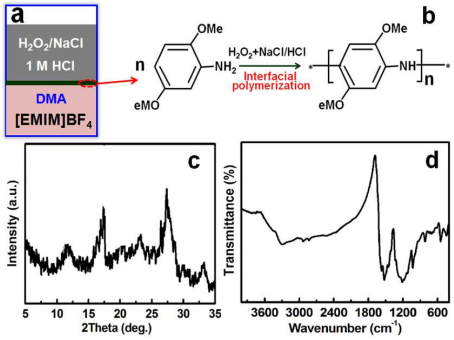

Fig. 1 Schematic illustration for the green interfacial synthesis (a) and polymerization process (b), XRD pattern (c), and FT-IR spectrum (d) of the resulting 2D PDMA NS product

The experimental details were systematically presented in Electronic Supporting Information (ESI†). Herein, an efficient green synthetic system, where the unique H_2O/[EMIM]BF_4 interface avoids the use of other poisonous organic solvents,

and much greener H_2O_2 was also used as even milder oxidant, was developed well for chemical oxidation polymerization of the PDMA, greatly facilitating its large-scale synthesis. Fig. 1c shows the typical powder X-ray diffraction (XRD) pattern of the as-prepared dark green PDMA product. Obviously, five diffraction peaks are evident at 2θ = 11.5º, 17º, 24º, 27º and 33º, and can be ascribed to the (001), (011), (100), (110) and (111) planes of the PDMA.[9] In specific, the former three peaks should be due to the presence of dopant anion Cl^- in the PDMA chains.[9] The peak centred at ~27º represents the characteristic distance between the ring planes of benzene rinds in adjacent chains or the close contact inter-chain distance, while the other one at ~33º may be attributed to the periodicity perpendicular to the polymer chain.[7] The Fourier transform infrared (FT-IR) spectrum of the resultant PDMA was also demonstrated in Fig. 1d. In specific, the peak at 1462 cm^{-1} is originated from asymmetrical bending vibration of $-OCH_3$ groups, and the bands at 1201 and 1025 cm^{-1} correspond to asymmetric and symmetric stretches of the =C-O-C, respectively, the three bands observed here obviously verify the existence of methoxy groups in the final PDMA NSs.[8] When other oxidants, such as, $FeCl_3$ or $(NH_4)_2S_2O_8$ (APS), are further used here for the interfacial polymerization, both PDMA products are obtained, as evident in the FT-IR spectra (Fig. S1, ESI†), and denoted as PDMA-$FeCl_3$ and PDMA-APS, respectively.

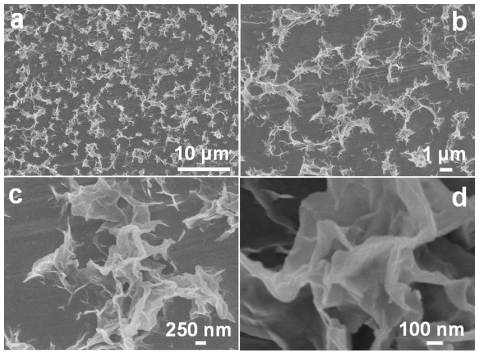

Fig. 2 FESEM (a-d) images of the as-obtained PDMA NSs

Fig. 2a-d show the representative field-emission scanning electron microscopy (FESEM) images of the resultant PDMA NS product. Evidently, a large scale of 2D NSs with rippled silk morphology, similar to graphene structure, are demonstrated, indicating the ultrathin nature of the PDMA NSs themselves. And it is due to the much larger lateral size than the longitudinal one, the morphology of bending, curling and crumpling is clearly presented. The thickness of the 2D NSs is estimated as ~20 nm, as shown in Fig. 2d. A large SSA is calculated as ~175 $m^2\ g^{-1}$ based on the N_2 adsorption-desorption measurement (Fig. S2, ESI†) for the as-obtained PDMA NS sample accordingly, owing to the unique 2D ultrathin feature. As a sharp contrast, just some nanoscale granular aggregations are shown for the PDMA synthesized *via* ordinary homogeneous synthesis (Fig. S3, ESI†). Of particular note, much thicker NSs with the thickness of ~50 nm are observed (Fig. S4, ESI†) when the NaCl is absent in the synthetic process. The abnormal phenomenon should be ascribed to the peculiar water/IL interface due to the lower ionic strength of water phase for this case. More interestingly, distinct irregular aggregation morphologies are further obviously presented for the PDMA-$FeCl_3$ and PDMA-APS samples (Fig. S5, ESI†). As a consequence, it is easy to conclude that the synergetic effect of the unique non-equilibrium water/IL interface and the appealing oxidant H_2O_2 plays an important role in the controllable synthesis of 2D PDMA NSs. And the inherent formation mechanism of such unique 2D PDMA still requires further study, which is currently under way.

To evaluate the electrochemical capacitive performance of the resultant PDMA NSs, cyclic voltammetry (CV) and chronopotentiometry (CP) were next carried out in 1 M HCl aqueous electrolyte at room temperature (RT). Fig. 3a shows the typical I-E response of the 2D PDMA NS electrode at a CV sweep rate of 2 mV s^{-1}. A pair of redox peaks within -0.2 - 0.3 V (*vs.* SCE) are obviously visible, and reveal that the typical pseudo-capacitive nature is mainly governed by inherent Faradaic redox reactions taking place on and/or near the surface of the 2D NSs. Impressively, the electrochemical response currents subsequently increase while the CV shape almost keeps the same with the increase of the scan rates, as demonstrated in the multi-scan rate voltammograms (Fig. 3b), suggesting good electrochemical capacitance of the unique PDMA NS electrode over the entire range of scan rates from 2 to 50 mV s^{-1}. Fig. 3c depicts the oxidation peak current of the as-prepared PDMA NSs as a function of the square root of scan rate ($v^{1/2}$). The linear relationship of I *vs.* $v^{1/2}$ shows a unique diffusion-control process.[14] The appealing conductivity (~0.07 S cm^{-1}) of the PDMA NSs may facilitate the rapid electron transfer rate, and thus the NS electrode process is rather a diffusion controlled than a kinetic one.[14] Additionally, galvanostatic CP test was then performed to estimate the SC of the PDMA NSs at a series of current densities ranged from 0.5 to 5 A g^{-1} in a potential window of -0.2 to 0.6 V (*vs.* SCE). The nonlinear CP plots with symmetric shape demonstrate striking pseudo-capacitive characteristics, as displayed in the CP curves of Fig. 3d. Noteworthy that high coulombic efficiency of >99% is delivered over all the current densities ranged from 0.5 to 5 A g^{-1}, as seen in Fig. 3d, revealing the desirable electrochemical reversibility of the PDMA NS electrode. The charge-discharge measurement is carried out in three consecutive cycles for each current density, and the SC finally is then calculated as a mean value of the former three cycles. Fig. 3e presents the SCs corresponding to different current densities in 1 M HCl aqueous solution. The SC of PDMA NSs is calculated as ~330 F g^{-1}, that is, an area specific SC of ~1.9 F m^2 considering its SSA, at a current density of 0.5 A g^{-1}, higher than that of the nanoscale PDMA electrode,[9] and even comparable to other CPs,[2, 3, 15] and 2D metal oxides,[16] sulphides[17] and selenides NSs.[18] Although the SC decrease of the PDMA NSs is observed with the increase of current density, a SC of ~286 F g^{-1} (*i.e.*, ~1.6 F m^2) still can be achieved even at a high current density of 5 A g^{-1}, which remains approximate to 87% of the highest SC value at 0.5 A g^{-1}. This further confirms the excellent high-rate performance of the PDMA NS electrode, which is of significant importance to its practical applications. Of particularly note, the SCs

delivered by the PDMA NS electrode are also much larger than those for PDMA-$FeCl_3$ (~221 F g^{-1} at 0.5 A g^{-1}) and PDMA-APS (~195 F g^{-1} at 0.5 A g^{-1}) samples (Fig. S6, ESI†), which should be ascribed to the smaller SSA for the PDMA-$FeCl_3$ (~101 m^2 g^{-1}) and PDMA-APS (~87 m^2 g^{-1}) products. Besides this, another important factor, modest electronic conductivities of the other two also must not be ignored. The conductivities of the PDMA-$FeCl_3$ and PDMA-APS products can be estimated as ~2×10^{-3} and ~6×10^{-3} S cm^{-1} *via* the standard four-probe DC technique on pressed pellets from powder, respectively, which can be further supported by different intersections of the electrochemical impedance spectroscopy (EIS) plots at the X-axis for the three PDMA electrodes (Fig. S7, ESI†). Finally, the PDMA NS electrode demonstrates even smaller charge-transfer resistance of ~0.4 ohm than the PDMA-$FeCl_3$ (~0.9 ohm) and PDMA-APS (~1.3 ohm) electrodes, estimated from the semicircle diameter observed at the high-medium frequency region (Fig. S7, ESI†), which also should be responsible for the large SCs of the unique 2D PDMA NS electrode, particularly at high rates.

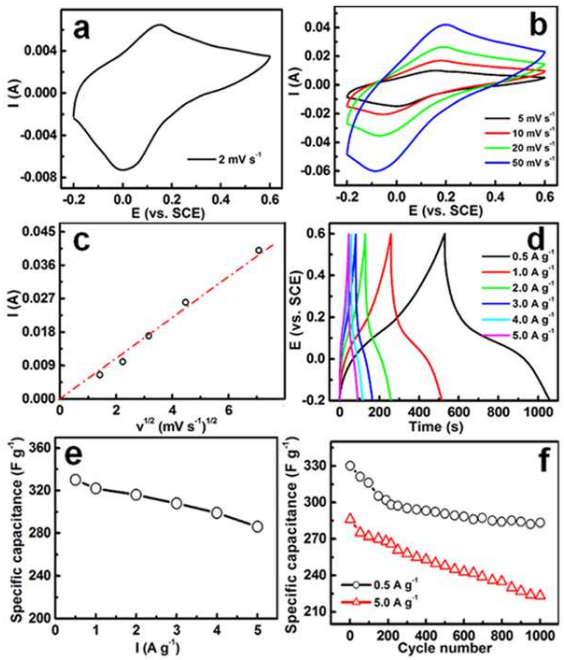

Fig. 3 CV curves (a, b), I *vs.* $v^{1/2}$ (c), CP plots (d), SC as a function of current density (e), and cycling performance (f) of the as-synthesized 2 D PDMA NSs

The long-term cycling stability is additionally critical requirement for practical ECs application. Fig. 3f depicts the SC variation as a function of the cycle number at current densities of 0.5 and 5 A g^{-1} for up to 1000 cycles. It can be detected that the SCs of the PDMA NS electrode gradually reduce, whereas the SC degradations of ~13% and ~22% are observed at 0.5 and 5 A g^{-1} over continuous 1000 cycles, indicating its stable long-term cycling performance even at large current density. As a contrast, the SC retentions of the two PDMA-$FeCl_3$ and PDMA-APS electrodes (Fig. S8, ESI†) are found as ~18% and ~23%, respectively, after continuous 1000 cycles at a current density of 0.5 A g^{-1}. The electrochemical data mentioned above strongly highlights the remarkable merits of the PDMA NSs as an advanced electrode to meet the requirements of both long cycling lifetime and large SCs at high rates, which should be attributed to the better electronic conductivity and smaller charge-transfer resistance of the 2D PDMA NSs with rich electroactive sites.

Furthermore, a quasi-supercapacitor is fabricated by using two PDMA NS electrodes face to face in 1 M HCl aqueous solution. The electrochemical performance of the PDMA NS-based symmetric supercapacitor is estimated and the typical data was collected (Fig. S9, ESI†). As seen from these typical CV curves (Fig. S9a, ESI†), the current subsequently increases as the scan rate increases while the CV shape changes little and rapid current response on voltage reversal occurs at each end potential, suggesting its appealing electrochemical capacitance. Additionally, based on the CP plots (Fig. S9b, ESI†), the SCs of the symmetric capacitor can be calculated as 78, 75 and 73 F g^{-1} at the current densities of 0.2, 0.5 and 1.0 A g^{-1}, respectively. And the specific energy density (E) and power density (P) of the PDMA NS-based symmetric capacitor are impressively calculated as ~3.7 Wh kg^{-1} and ~304.1 W kg^{-1} at a current density of 1.0 A g^{-1}.

In summary, we have successfully developed an attractive green interfacial strategy to synthesize 2D PDMA NSs herein, and further applied it as a high performance pseudo-capacitive electrode for ECs. Benefiting from the intriguing 2D NS feature, high electronic conductivity and modest charge-transfer resistance, the as-fabricated PDMA NS electrode delivered large SCs, and stabilized cycling performance coupled with high coulombic efficiency in 1 M HCl aqueous solution. More significantly, an efficient green avenue is now open for future development of other low-cost electroactive materials for next-generation ECs.

This work was supported by the National Natural Science Foundation of China (no. 51202004), the Natural Science Foundation of Anhui Province (KJ2013A051), and the Opening Project of CAS Key Laboratory of Materials for Energy Conversion (no. 2014001).

Notes and references

[a] *School of Materials Science and Engineering, Anhui University of Technology, Ma'anshan, 243002, P. R. China*
Email:ayuancz@163.com
[b] *Department of Chemistry, College of Chemistry and Chemical Engineering, Xiamen University, Xiamen, 361005, P. R. China*
Email:jdlin@xmu.edu.cn
[c] *Chinese Academy of Science (CAS) Key Laboratory of Materials for Energy Conversion, Hefei, 230026, P. R. China*

† Electronic Supplementary Information (ESI) available: [The detailed synthesis condition, materials and characterizations]. See DOI: 10.1039/b000000x/

1 C. Liu, F. Li, L. P. Ma and H. M. Cheng, Adv. Mater., 2010, **22**, E28; C. Z. Yuan, H. B. Wu, Y. Xie and X. W. Lou, *Angew. Chem. Int. Ed.*, 2014, **53**, 1488; P. Simon and Y. Gogotsi, *Nat. Mater.*, 2008, **7**, 845; B. E. Conway, *Electrochemical Supercapacitors: Scientific Fundamentals and Technological Applications*, Kluwer Academic/Plenum Publishers, New York, 1999.
2 C. Z. Yuan, L. R. Hou, L. F. Shen and X. G. Zhang, *J. Electrochem. Soc.*, 2012, **159**, A1323.
3 L. R. Hou, C. Z. Yuan, D. K. Li, L. Yang, L. F. Shen, F. Zhang and X. G. Zhang, *Electrochim. Acta*, 2011, **56**, 6049; X. J. Lu, H. Dou, C. Z.

Yuan, S. D. Yang, L. Hao, F. Zhang, L. F. Shen, L. J. Zhang and X. G. Zhang, *J. Power Sources*, 2012, **197**, 319.
4 Q. Wang, J. Yan, Z. J. Fan, T. Wei, M. L. Zhang and Y. Y. Jing, *J. Power Sources*, 2014, **247**, 197; C. Z. Yuan, L. F. Shen, X. J. Lu and X. G. Zhang, *Chem. Lett.*, 2010, **39**, 850.
5 S. E. Mavundla, G. F. Malgas, P. Baker and E. I. Iwuoha, *Electroanalysis*, 2008, **20**, 2347.
6 R. D. Calleja, E. S. Matveeva and V. P. Parkhutik, *J. Non-Cryst. Solids*, 1995, **180**, 260; A. J. Epstein and A. G. MacDiarmid, *Macromol. Symp.*, 1991, **51**, 217.
7 L. M. Huang, T. C. Wen and A. Gopalan, *Mater. Lett.*, 2003, **57**, 1765; G. D. Storrier, S. B. Colbran and D. B. Hibbert, *Synth. Met.*, 1994, **62**, 179; G. D. Aprano, M. Leclerc, G. Zptti and G. Schiavon, *Chem. Mater.*, 1995, **7**, 33.
8 A. Muslim, T. Abdryim and S. Zhi, *Polym. Sci.*, 2011, 53, 480.
9 S. P. Palaniappan, S. R. P. Gnanakan, Y. S. Lee and P. Manisamkar, *Ionics*, 2011, 1**7**, 603.
10 S. Jain, S. P. Surwade, S. R. Agnihotra, V. Dua, P. A. Eliason, G. J. Morose and S.K. Manohar, *Green Chem.*, 2010, **12**, 585.
11 J. X. Huang, S. Virji, B. H. Weiller and R. B. Kaner, *J. Am. Chem. Soc.*, 2003, **125**, 314.
12 J. H. Zhu, M. J. Chen, H. L. Qu, X. Zhang, H. G. Wei, Z. P. Luo, H. A. Colorado, S. Y. Wei and Z. H. Guo, *Polymer*, 2012, **53**, 5953; J. G. Wang, Y. Yang, Z. H. Huang and F. Y. Kang, *J. Power Sources*, 2012, **204**, 236; H. Y. Ma, Y. Q. Luo, S. X. Yang, Y. W. Li, F. Cao and J. Gong, *J. Phys. Chem. C*, 2011, **115**, 12048.
13 L. R. Hou, Q. Zhang, L. T. Ling, C. X. Li and S. Chen, *J. Am. Chem. Soc.*, 2013, **135**, 10618; S. Y. Yang, C. F. Wang and S. Chen, *J. Am. Chem. Soc.*, 2011, **133**, 8412; L. R. Hou, L. Lian, L. H. Zhang, T. Wu and C. Z. Yuan, *RSC Adv.*, 2014, **4**, 2374; C. Z. Yuan, L. R. Hou, L. Yang, D. K. Li, L. F. Shen, F. Zhang and X. G. Zhang, *J. Mater. Chem.*, 2011, **21**, 16305.
14 Y. G. Wang, Z. S. Hong, M. D. Wei and Y. Y. Xia, *Adv. Funct. Mater.*, 2012, **22**, 5185; Y. Wang, C. X. Guo, J. H. Liu, T. Chen, H. B. Yang and C. M. Li, *Dalton Trans.*, 2011, **40**, 6388.
15 M. J. Bleda-Martínez, C. Peng, S. G. Zhang, G. Z. Chen, E. Morallón and D. Cazorla-Amorós, *J. Electrochem. Soc.*, 2008, **155**, A672; D. W. Wang, F. Li, J. P. Zhao, W. C. Ren, Z. G. Chen, J. Tam, Z. S. Wu, L. Gentle, G. Q. Lu and H. M. Cheng, *ACS Nano*, 2009, **3**, 1745.
16 C. Z. Yuan, L. Yang, L. R. Hou, L. F. Shen, X. G, Zhang, X. W. Lou, *Energy Environ. Sci.*, 2012, **5**, 7883.
17 C. L. Zhang, H. H. Yin, M. Han, Z. H. Dao, H. Pang, Y. L. Zheng, Y. Q. Lan, J. C. Bao and J. M. Zhu, *ACS Nano*, 2014, **8**, 3761
18 J. Feng, X. Sun, C. Xu, C. Lin, S. Hu, J. Yang, Y. Xie, *J. Am. Chem. Soc.*, 2011, **133**, 17832.